Biophysical Chemistry, 30 (1988) 271–277
Elsevier

BPC 01264

Detection of three rotational correlation times for a rigid asymmetric molecule using frequency-domain fluorometry

Ignacy Gryczynski, Henryk Cherek and Joseph R. Lakowicz

University of Maryland at Baltimore, School of Medicine, Department of Biological Chemistry, 660 West Redwood Street, Baltimore, MD 21201, U.S.A.

Received 27 January 1988
Accepted 23 March 1988

Frequency-domain fluorometry; Rotational diffusion; Fluorescence; Anisotropy decay; Polarization

We measured the frequency response of the polarized emission of Y_t-base in propylene glycol at 10 °C. Data were obtained for excitation wavelengths of 290, 312 and 346 nm, for which the fundamental anisotropies are 0.05, 0.19 and 0.32, respectively. Additionally, data were obtained using CCl_4, to decrease the mean decay time from 9.1 to 4.2 ns. These nine sets of data were analyzed globally to recover the anisotropy decay law. Three correlation times were needed to fit the data, 0.8, 3.0 and 5.6 ns, a range of only 7-fold. We believe this is the first reported detection of three correlation times for a rigid molecule.

1. Introduction

Fluorescence anisotropy decays depend upon the size, shape and optical properties of the rotating molecule [1–3]. Ellipsoids of revolution can display two rotational correlation times, and three correlation times are possible for asymmetric molecules. To the best of our knowledge, three correlation times have not yet been detected for an asymmetric molecule, presumably because of the difficulty in obtaining data with adequate information content and signal-to-noise ratio.

We examined Y_t-base (Y-4,9-dihydro-4,6-dimethyl-9-oxo-1*H*-1-imidazo-1,2*a*-purine) because its structure is asymmetric (scheme 1) and the absorption and emission moments are probably not directed along the principle axes [4]. Anisotropy data were measured in the frequency domain, which provides good resolution of rapid or closely spaced correlation times [5–7]. To obtain enhanced information content we performed doubly global measurements and analyses. First, the data were obtained using different excitation wavelengths, thereby varying the fundamental anisotropy from 0.05 to 0.32. In this way we altered the orientation of the absorption moment within the molecular axis, and thus altered the contribution of rotations about each axis to the anisotropy data [8]. Secondly, we varied the mean decay time using CCl_4 as a collisional quencher. As the lifetime is decreased the early time portion of the anisotropy decay contributes increasingly to the data [9]. These nine data sets (three wavelengths and three quencher concentrations) were analyzed

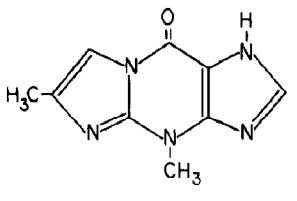

Scheme 1. Chemical structure of the Y_t-base.

Correspondence address: J.R. Lakowicz, University of Maryland at Baltimore, School of Medicine, Department of Biological Chemistry, 660 West Redwood Street, Baltimore, MD 21201, U.S.A.

by a global least-squares algorithm to recover three correlation times.

2. Theory and analysis

The anisotropy decay at each excitation wavelength (λ) can be described by

$$r^{\lambda}(t) = \sum_i r_{0i}^{\lambda} \exp(-t/\theta_i) \tag{1}$$

where λ indicates the excitation wavelength and θ_i are the correlation times. The values of r_{0i}^{λ} represent the amplitude of the anisotropy which decays via the i-th correlation time when using an excitation wavelength λ. It should be noted that the correlation times are related to, but not equal to, the rotational diffusion coefficients of the fluorophore about the principle axes [1–3,10]. In our analyses the individual r_{0i}^{λ} values were all variable parameters. If the data are adequate to recover the entire anisotropy decay then one expects the $\Sigma_{\lambda} r_{0i}$ to equal r_0^{λ}, where r_0^{λ} is the anisotropy measured in the absence of rotational diffusion, i.e., under frozen or vitrified conditions. The values of r_0^{λ} depend upon the average angle between the absorption and emission transition moments at each excitation wavelength. This dependence in turn alters the relative contribution of each rotational motion to the anisotropy decay [11].

In the frequency domain the measured quantities are the phase angle difference between the parallel ($\|$) and perpendicular ($\perp$) components of the emission ($\Delta_{\omega}^{\lambda q} = \phi_{\perp} - \phi_{\|}$) and the ratio of the polarized and modulated components of the emission ($\Lambda_{\omega}^{\lambda q} = m_{\|}/m_{\perp}$), each measured over a range of modulation frequencies (ω), wavelengths (λ) and quencher concentrations (q). For purposes of nonlinear least-squares analysis the calculated values (c) are obtained using

$$\Delta_{c\omega}^{\lambda q} = \arctan\left(\frac{D_{\|}^{\lambda q} N_{\perp}^{\lambda q} - N_{\|}^{\lambda q} D_{\perp}^{\lambda q}}{N_{\|}^{\lambda q} N_{\perp}^{\lambda q} + D_{\|}^{\lambda q} D_{\perp}^{\lambda q}}\right), \tag{2}$$

$$\Lambda_{c\omega}^{\lambda q} = \left(\frac{\left(N_{\|}^{\lambda q}\right)^2 - \left(D_{\|}^{\lambda q}\right)^2}{\left(N_{\perp}^{\lambda q}\right)^2 + \left(D_{\perp}^{\lambda q}\right)^2}\right)^{1/2} \tag{3}$$

where

$$N_i^{\lambda q} = \int_0^{\infty} I_i^{\lambda q}(t) \sin \omega t \, \mathrm{d}t, \tag{4}$$

$$D_i^{\lambda q} = \int_0^{\infty} I_i^{\lambda q}(t) \cos \omega t \, \mathrm{d}t \tag{5}$$

and i represents the parallel or perpendicular component of the emission. These components of the emission are given by

$$I_{\|}^{\lambda q}(t) = \tfrac{1}{3} I_0^{\lambda q}(t)\left[1 + 2r^{\lambda}(t)\right], \tag{6}$$

$$I_{\perp}^{\lambda q}(t) = \tfrac{1}{3} I_0^{\lambda q}(t)\left[1 - r^{\lambda}(t)\right], \tag{7}$$

where $I_0^{\lambda q}(t)$ is the decay of the total emission. The goodness-of-fit to the anisotropy decay law (eq. 1) is estimated from the value of reduced chi-squared,

$$\chi_R^2 = \frac{1}{\nu} \sum_{\omega,\,\lambda,\,q} \left(\frac{\Delta_{\omega}^{\lambda q} - \Delta_{c\omega}^{\lambda q}}{\delta\Delta}\right)^2 + \frac{1}{\nu} \sum_{\omega,\,\lambda,\,q} \left(\frac{\Lambda_{\omega}^{\lambda q} - \Lambda_{c\omega}^{\lambda q}}{\delta\Lambda}\right)^2, \tag{8}$$

where ν is the number of degrees of freedom (number of data points minus number of floating parameters), and $\delta\Delta$ and $\delta\Lambda$ denote the uncertainties in the measured values. In the present paper the data at all ω, λ and q are analyzed simultaneously to recover a single set of correlation times, and three sets of amplitudes (r_{0i}), one set for each excitation wavelength. This analysis may be regarded as an extension of the global analyses suggested by Brand and co-workers [12,13], which includes an extension to anisotropy decays with multiple excitation wavelengths [8] and quencher concentrations [9].

The modulation data are presented as the modulated anisotropy

$$r_{\omega}^{\lambda q} = \left(\Lambda_{\omega}^{\lambda q} - 1\right)/\left(\Lambda_{\omega}^{\lambda q} + 2\right). \tag{9}$$

The values of $r_{\omega}^{\lambda q}$ are comparable to those of the steady-state anisotropy ($r^{\lambda q}$) and the fundamental anisotropy r_0^{λ}. At low modulation frequencies $r_{\omega}^{\lambda q}$ is nearly equal to $r^{\lambda q}$. At high modulation frequencies $r_{\omega}^{\lambda q}$ approaches r_0^{λ} [14,15].

It should be noted that the intensity decays of Y_t-base become increasingly heterogeneous in the

presence of quencher. This is due to transient effects in translational diffusion [16,17]. The rotation-free intensity decays were measured at each excitation wavelength and quencher concentration. The data were fitted to the multiexponential model [18,19],

$$I_0^{\lambda q}(t) = \sum_i \alpha_i^{\lambda q} e^{-t/\tau_i^{\lambda q}} \qquad (10)$$

The parameters from the double- or triple-exponential fit were used in eqs. 6 and 7. These parameters ($\alpha_i^{\lambda q}$ and $\tau_i^{\lambda q}$) were, as expected, strongly dependent on the quencher concentration. Nearly equivalent values were obtained for each excitation wavelength for the same concentration of quencher.

3. Materials and methods

Frequency-domain measurements were performed using the 2 GHz fluorometer described previously [20]. This instrument was modified by addition of a second dye laser for pyridin 2. After frequency doubling, this dye provided excitation at 346 nm. The frequency-doubled output of rhodamine 6G was used for excitation at 312 and 290 nm.

All solutions were in propylene glycol at 10 °C. Y_t-base was purified by HPLC. The laser beam was expanded to about 5 mm diameter to decrease its local intensity. The emission was observed through a Corning 3-74 filter. We did not notice any significant loss of intensity or changing phase or modulation values during the experiment, suggesting that photodecomposition was not significant.

4. Results

The absorption and emission spectra of Y_t-base are shown in fig. 1, as is the excitation anisotropy spectrum in vitrified solution (−60 °C). We chose three excitation wavelengths, 290, 312 and 346 nm. As indicated by the arrows these wavelengths yield r_0 values of 0.05, 0.19 and 0.32, respectively.

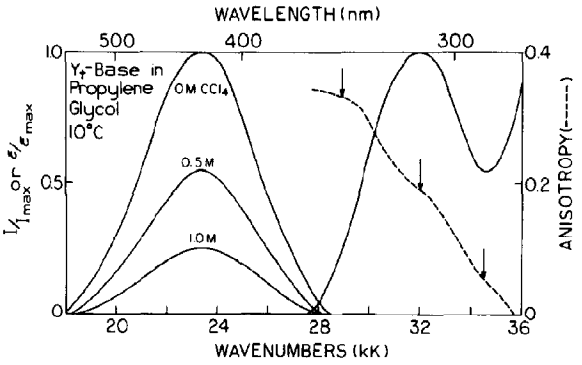

Fig. 1. Absorption, emission and anisotropy spectra of Y_t-base. The anisotropy values (r_0^{λ}) were measured at −60 °C.

The emission was quenched by CCl_4, resulting in about 50 and 75% quenching at 0.5 and 1.0 M CCl_4, respectively.

Frequency-domain intensity data are shown in fig. 2, in the absence (●) and presence (○) of 1 M CCl_4. In the absence of CCl_4 the intensity decay is a weak double exponential, and is not badly fitted by a single exponential ($\chi_R^2 = 24$). In the presence of quenching the decay becomes strongly

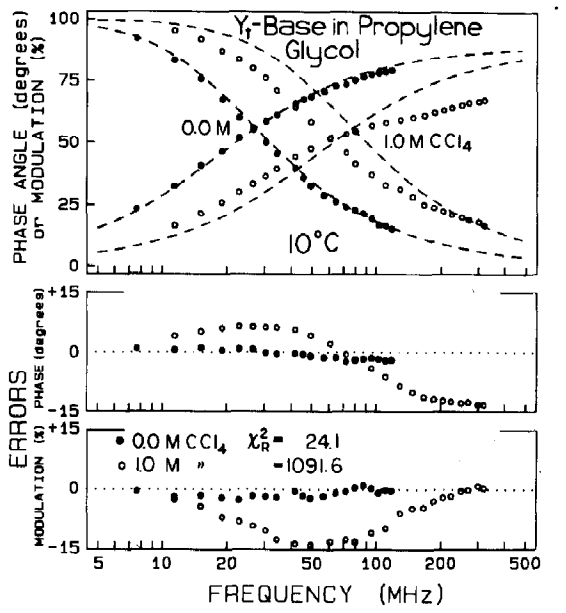

Fig. 2. Frequency response of the emission of Y_t-base, with (○) and without (●) 1 M CCl_4. The dashed lines show the best single-decay-time fit to the data.

Table 1

Intensity decays of Y_t-base

Excitation wavelength (nm)	$[CCl_4]$ (M)	$\alpha_i^{\lambda q}$	$f_i^{\lambda q}$ [a]	$\tau_i^{\lambda q}$ (ns)	$\bar{\tau}$ (ns) [b]	χ_R^2
290	0	1	1	8.61		32.8
		0.116	0.023	1.66		
		0.884	0.977	9.25	9.08	1.7
290	0.5	1	1	4.82		558.3
		0.412	0.085	0.84		
		0.588	0.915	6.34	5.87	1.8
290	1.0	1	1	3.01		1131.2
		0.531	0.120	0.56		
		0.469	0.880	4.68	4.19	2.4
312	0	1	1	8.66		28.1
		0.107	0.020	1.59		
		0.893	0.980	9.23	9.08	1.1
312	0.5	1	1	4.84		533.1
		0.404	0.083	0.84		
		0.596	0.917	6.32	5.86	1.3
312	1.0	1	1	3.04		1122.6
		0.528	0.118	0.56		
		0.472	0.882	4.69	4.20	1.9
346	0	1	1	8.67		24.7
		0.100	0.019	1.65		
		0.900	0.981	9.21	9.07	1.8
346	0.5	1	1	4.87		516.1
		0.398	0.081	0.84		
		0.602	0.919	6.31	5.87	2.0
346	1.0	1	1	3.06		1091.6
		0.522	0.116	0.56		
		0.478	0.884	4.69	4.21	1.6

[a] The fractional intensities ($f_i^{\lambda q}$) are given by $f_i^{\lambda q} = \alpha_i^{\lambda q}\tau_i^{\lambda q}/\sum\alpha_i^{\lambda q}\tau_i^{\lambda q}$.

[b] The mean decay times were calculated using $\bar{\tau} = f_1\tau_1 + f_2\tau_2$.

heterogeneous, and cannot even be approximately fitted using the single-exponential model ($\chi_R^2 = 1092$). We parameterized each intensity decay using a double-exponential model (table 1). The intensity decays become increasingly heterogeneous with quenching, as can be judged by the increases in χ_R^2 for the single-decay-time fits. It should be noted that the intensity decays are not significantly dependent upon excitation wavelength. For each quencher concentration essentially the same intensity decay parameters are found ($\alpha_i^{\lambda q}$ and $\tau_i^{\lambda q}$) for each excitation wavelength.

Frequency-domain anisotropy data are shown in fig. 3. The values are seen to depend upon both the excitation wavelength and quencher concentration. The most dramatic change is caused by variations in the excitation wavelength, with more modest differences at each quencher concentration. At low modulation frequencies (5–20 MHz) the modulated anisotropies ($r_\omega^{\lambda q}$) increase with $[CCl_4]$, reflecting an increase in the steady-state anisotropy. At high modulation frequencies the $r_\omega^{\lambda q}$ values tend toward the r_0^λ value for each excitation wavelength. The phase angles decrease with increasing concentrations of CCl_4.

The data in fig. 3 were analyzed globally to recover one, two or three correlation times (table 2). The portion of the total anisotropy associated with each correlation time was a variable parameter. Hence, the analysis yields three r_{0i}^λ values for each correlation time, one for each excitation wavelength. Also, the analysis yielded three corre-

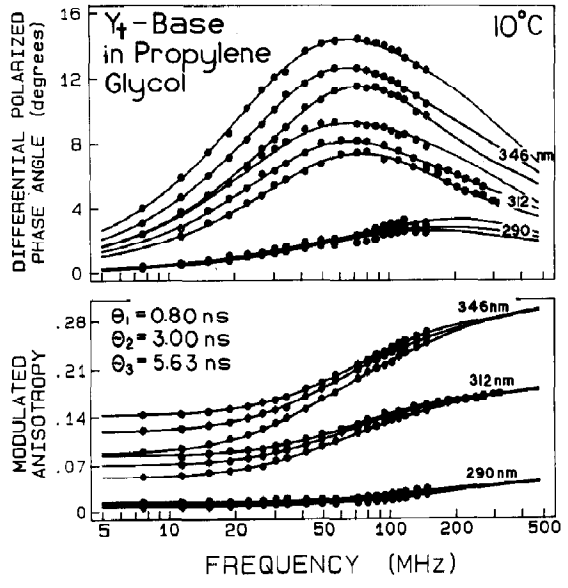

Fig. 3. Frequency-domain anisotropy data for Y_t-base. In the upper panel, at each excitation wavelength, the decreasing phase angles are for 0, 0.5 and 1.0 M CCl_4. In the lower panel, at each excitation wavelength, the increasing modulated anisotropies are for 0, 0.5 and 1.0 M CCl_4.

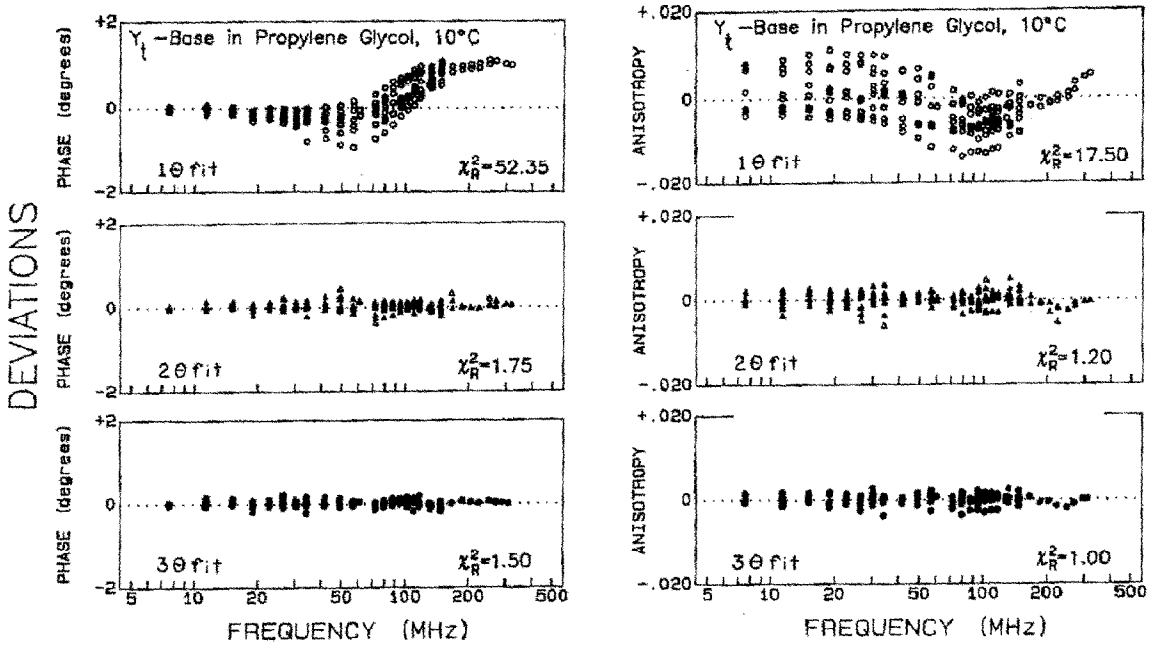

Fig. 4. Deviations between the measured and calculated Δ_ω (left) and Λ_ω (right) values. The χ^2_R values are those for either the Δ_λ or Λ_ω measurements, but the fits were obtained by simultaneous fitting to both Δ_ω and Λ_ω.

lation times and three amplitudes for each excitation wavelength. For the three-correlation-time analysis 12 parameters are recovered (nine r_{0i} and three θ_i values). The data could not be fitted using the single-correlation-time model, as is seen from $\chi^2_R = 34.6$ (table 2). The inadequacy of the single-correlation-time fit is also evident from the large and systematic deviations between the measured and calculated values of Δ_ω and Λ_ω (fig. 4). The use of two correlation times results in a 24-fold decrease in χ^2_R (table 2) and in more random deviations (fig. 4). A further decrease of 1.45-fold in χ^2_R was found using three correlation times and the deviations appear to be somewhat smaller and more random. With 128 data points and 12 variable parameters there are 116 degrees of freedom. For random deviations in the data, and $\nu = 116$, a 1.45-fold increase in χ^2_R is expected less than 1% of the time. Hence, the data almost certainly indicate the need to accept the model with three correlation times.

Table 2

Global analysis of the anisotropy decay of Y_t-base

Model [a]	θ_i (ns)	r_{0i}			χ^2_R
		296 nm	312 nm	346 nm	
1θ	3.37	0.037	0.176	0.286	34.55
2θ	0.99	0.040	0.067	0.096	
	4.91	0.007	0.125	0.216	1.45
Σr^λ_{0i}		0.047	0.192	0.312	
3θ	0.80 (0.02) [b]	0.042	0.048	0.78	
	3.00 (0.08)	0.000	0.068	0.85	
	5.63 (0.08)	0.009	0.076	0.152	0.99
Σr^λ_{0i}		0.51	0.192	0.315	
Measured r_0		0.05	0.19	0.32	

[a] 1θ is the fit to one correlation time, etc.

[b] Uncertainties in θ_i from the diagonal elements of the covariance matrix [22].

Our confidence in the analysis is enhanced by recovery of the expected values for the total anisotropy ($\Sigma_\lambda r^\lambda_{0i}$). At each excitation wavelength the Σr^λ_{0i} was found to equal the value of r^λ_0 measured in frozen solution. It should also be noted that the correlation times are closely spaced, and span only

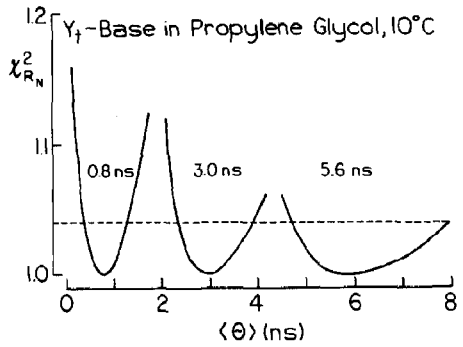

Fig. 5. χ^2_R surface for the three correlation times of Y_t-base.

a range of 7-fold, i.e., 0.8, 3.0 and 5.6 ns. To the best of our knowledge, this is the first measurement of three correlation times for a rigid molecule. Sasaki et al. [21] suggested that three diffusion coefficients were detected for perylene, but their analysis used fixed r_{0i}^{λ} values, and only two correlation times appear to have been recovered from the data.

Finally, we questioned the uncertainties in the correlation times. One estimate of the uncertainty is provided from the least-squares analysis, and in particular from the diagonal elements of the covariance matrix [22]. These values are correct only if there is no correlation between the fitted parameters. These uncertainty estimates are near 0.05 ns (table 2), so that the three correlation times, with their associated uncertainties, do not overlap. However, the parameters are correlated, so that 50 ps is a minimum value for the uncertainty.

We performed a more vigorous analysis of the correlation time uncertainties. We examined the values of χ^2_R as each correlation time was varied about the value yielding the χ^2_R minimum (fig. 5). Using this fixed value the least-squares analysis was performed again, allowing the remaining correlation times and all the amplitudes to vary, yielding the minimum value of χ^2_R consistent with the fixed correlation time. Since all the other parameters vary during reanalysis, this procedure should account for all correlations between the parameter values. The dashed line in fig. 5 indicates the value of χ^2_R expected 33% of the time due to random errors. For lack of a vigorous theory for uncertainties, we take this elevation in χ^2_R as defining the uncertainty in the correlation times. Using this approach the θ_i values have an uncertainty of about $\pm 50\%$. However, the χ^2_R surfaces do not overlap within the uncertainty limits, which indicates the necessity of at least three correlation times to account for the data. We believe that this method overestimates the uncertainties in the correlation times by about 2-fold.

5. Discussion

What are the origins of the three correlation times for Y_t-base? Three correlation times are possible for an asymmetric molecule, if the absorption and emission moments are not directed along a principle axis of the molecule [1]. It should also be noted that these expressions for rotational diffusion [1–3] are only appropriate for the stick boundary conditions, i.e., when the rotating molecule feels the solvent viscosity for each rotational motion. For small molecules in solution, especially those with no sites for hydrogen bonding, the molecule can slip (not feel the solvent viscosity) about one or more of its axes [23,24]. Hence, for Y_t-base the three correlation times may originate from either its asymmetric structure or partial slipping about one or more axes.

It is also desirable to interpret the correlation times and amplitudes in terms of the structure, rotational rates about the molecular axes and the orientation of the absorption and emission axes. At present, this analysis is incomplete, and we do not know if an unambiguous interpretation will be possible.

Acknowledgements

This work was supported by grants DMB-8502835 and DMB-8511065 from the National Science Foundation, and grant GM 39617 from the National Institutes of Health.

References

1 G.G. Belford, R.L. Belford and G. Weber, Proc. Natl. Acad. Sci. U.S.A. 69 (1972) 1392.

2 E.W. Small and I. Isenberg, Biopolymers 16 (1977) 1907.
3 T.J. Chuang and K.B. Eisenthal, J. Chem. Phys. 57 (1972) 5094.
4 I. Gryczynski, Z. Gryczynski, A. Kawaski and S. Paszyc, Photochem. Photobiol. 39 (1984) 319.
5 J.R. Lakowicz and B.P. Maliwal, Biophys. Chem. 21 (1985) 61.
6 J.R. Lakowicz, G. Laczko and I. Gryczynski, Biochemistry 26 (1987) 82.
7 B.P. Maliwal and J.R. Lakowicz, Biochim. Biophys. Acta 873 (1986) 161.
8 I. Gryczynski, H. Cherek, G. Laczko and J.R. Lakowicz, Chem. Phys. Lett. 135 (1987) 193.
9 J.R. Lakowicz, H. Cherek, I. Gryczynski, N. Joshi and M.L. Johnson, Biophys. J. 51 (1987) 755.
10 M.D. Barkley, A. Kowalczyk and L. Brand, J. Chem. Phys. 75 (1981) 3581.
11 G. Weber, J. Chem. Phys. 66 (1977) 4081.
12 J.R. Knutson, J.M. Beechem and L. Brand, Chem. Phys. Lett. 1–2 (1983) 501
13 J.M. Beechem, J.R. Knutson, J.B.A. Ross, B.J. Turner and L. Brand, Biochemistry 22 (1983) 6054.
14 B.P. Maliwal and J.R. Lakowicz, Biochim. Biophys. Acta 873 (1986) 161.
15 B.P. Maliwal, A. Hermetter and J.R. Lakowicz, Biochim. Biophys. Acta 873 (1986) 173.
16 J.R. Lakowicz, M.L. Johnson, I. Gryczynski, N. Joshi and G. Laczko, J. Phys. Chem. 91 (1987) 3277.
17 N. Joshi, M.L. Johnson and J.R. Lakowicz, Chem. Phys. Lett. 135 (1987) 200.
18 J.R. Lakowicz, E. Gratton, G. Laczko, H. Cherek and M. Limkeman, Biophys. J. 46 (1984) 463.
19 E. Gratton, J.R. Lakowicz, B. Maliwal, H. Cherek, G. Laczko and M. Limkeman, Biophys. J. 46 (1984) 479.
20 J.R. Lakowicz, G. Laczko and I. Gryczynski, Rev. Sci. Instrum. 57 (1986) 2499.
21 T. Sasaki, K. Hiroto, M. Yamamato and Y. Nishijima, Bull. Chem. Soc. Jap. 60 (1987) 1165.
22 P.R. Bevington, Data reduction and error analysis for the physical sciences (McGraw Hill, New York, 1969) p. 242, 313.
23 C.M. Yu and R. Zwanzig, J. Chem. Phys. 60 (1974) 4354.
24 G.K. Youngren and A. Acrivor, J. Chem. Phys. 63 (1975) 3846.